Bis[*O*-methyl (*S*)-penicillaminato]-*cis*-dioxomolybdenum(VI), $[MoO_2\{(S)\text{-pen-OMe}\}_2]$; Structure and Spectroscopic Studies †

Iain Buchanan and C. David Garner *
The Chemistry Department, Manchester University, Manchester M13 9PL
William Clegg *
Anorganisch-Chemisches Institut der Universität Göttingen, Tammannstrasse 4, D3400 Göttingen, Federal Republic of Germany

The complex $[MoO_2\{(S)\text{-pen-OMe}\}_2]$ crystallises in the monoclinic space group $P2_1$, with a = 11.794(2), b = 12.519(3), c = 13.040(2) Å, β = 106.32(2)°, and Z = 4. The structure was solved from 5 502 unique observed reflections, and refinement gave a final R of 0.039; anomalous dispersion was employed to verify the absolute configuration at molybdenum and at the chiral carbon of the ligands. The two crystallographically independent molecules have opposite absolute configurations (Λ and Δ) for the ligand chelate rings about the metal; the expected *cis*-dioxo-stereochemistry is confirmed, with normal bond lengths [average Mo–O 1.712(7), Mo–S 2.407(5), and Mo–N 2.362(26) Å]. Proton, ^{13}C, and ^{95}Mo n.m.r. spectra are consistent with these two diastereoisomeric molecules persisting in solution, and together with c.d. data are taken to indicate that, for the (*S*)-ligand complex in $(CD_3)_2SO$ at *ca.* 298 K, the Λ isomer is present in a *ca.* 2:1 excess over the Δ isomer, the reverse being the case for the (*R*)-ligand complex. The two diastereoisomers are in dynamic equilibrium and ^1H n.m.r. data collected over the temperature range 297—385 K indicate that the activation parameters for the Λ ⟶ Δ interconversion are $\Delta H^{\ddagger}$ = 44 ± 6 kJ mol^{-1} and $\Delta S^{\ddagger}$ = −110 ± 17 J K^{-1} mol^{-1}. The mechanism for the inversion of configuration at molybdenum is considered to proceed by an intramolecular process, involving Mo–N bond rupture followed by rotation of the ligand atoms of the subsequent intermediate and ring closure. C.d. spectra resolve each of the u.v.–visible absorption bands centred at *ca.* 264 and 352 nm into two components. The i.r. active ν(Mo–O_t) stretching vibrations of *cis*-$[MoO_2\{(S)\text{-pen-OMe}\}_2]$ are manifest as a pair of doublets at 918/913 and 878/875 cm^{-1}, presumably due to the Λ and Δ isomers having slightly different ν(Mo–O_t) values.

The structural, spectroscopic, and chemical properties of oxomolybdenum complexes are important, not only in their own right but also to consolidate and extend the knowledge available for a satisfactory interpretation of the structure and function of the molybdenum centres in the oxomolybdoenzymes, *viz.* sulphite, xanthine, and aldehyde oxidase and nitrate reductase.[1-4] As part of an on-going study of oxomolybdenum complexes,[5-9] we have prepared and characterised the complexes of *cis*-dioxomolybdenum(VI) with the (*R*)- and (*S*)-enantiomers of penicillamine *O*-methyl ester. Complexes of this type are of interest in that they involve a similar set of ligand donor atoms (two terminal oxo-groups and two sulphur atoms) to those reported for molybdenum(VI) in sulphite oxidase,[10] on the basis of molybdenum *K*-edge extended *X*-ray absorption fine structure (EXAFS) studies. The spectroscopic characterisation of these complexes is of value, especially with reference to the circular dichroism (c.d.) and Raman spectra of rat liver sulphite oxidase.[7,9] Also, the kinetics and mechanism of inversion of the configuration about molybdenum, reported and discussed herein, may be pertinent to the substitutional reactivity of *cis*-dioxomolybdenum(VI) centres, including those of the oxomolybdoenzymes.

Experimental

Preparation of (R)- *and* (S)-*Penicillamine Methyl Ester Hydrochlorides*.—These preparations were carried out under anhydrous, anaerobic conditions, using the appropriate enantiomer of penicillamine; (*R*)-penicillamine was obtained from Sigma and (*S*)-penicillamine from Aldrich. To a solution of penicillamine (1.51 g, 10.1 mmol) in methanol (30 cm^3) was added an excess of freshly distilled thionyl chloride (3.0 cm^3). The vessel was sealed and the reaction mixture was stirred for 4—5 d, after which time the volume was reduced under vacuum to *ca.* 15 cm^3. The volume was then made up to 100 cm^3 with diethyl ether, thereby producing a white crystalline precipitate of the penicillamine ester hydrochloride, which was isolated by filtration and washed with diethyl ether (2 × 20 cm^3) before drying under vacuum. The yield was 75% (1.50 g, 7.51 mmol) and the product was characterised by ^1H n.m.r. and i.r. spectroscopy. Each ^1H n.m.r. spectrum contained resonances due to the amine protons (7.3 p.p.m., br s), the α-CH proton (4.10 p.p.m., br s), the methyl ester group (1.90 p.p.m., s), and the two C_β–CH_3 groups (singlets at 1.24 and 1.51 p.p.m.) with the correct relative intensities. Each i.r. spectrum exhibited a single ν(C=O) vibration at 1 740 cm^{-1} and a ν(S–H) mode at 2 520 cm^{-1}. The materials were used without further purification.

Preparation of Bis[O-*methyl* (S)-*penicillaminato*]-cis-*dioxomolybdenum*(VI), $[MoO_2\{(S)\text{-pen-OMe}\}_2]$.—The complex was prepared by a method analogous to that used for $[MoO_2\{(R)\text{-cys-OR}\}_2]$ (cys-OR = deprotonated cysteine ester, R = Me or Et).[11,12] (*S*)-Penicillamine methyl ester hydrochloride (0.68, 3.41 mmol) was dissolved in water (15 cm^3) and added with stirring to a solution of $Na_2[MoO_4]\cdot 2H_2O$ (0.50 g, 2.07 mmol) in water (20 cm^3), to give an immediate bright yellow precipitate. After stirring for 30 min, the product was isolated by filtration and washed with water (2 × 15 cm^3), 95% ethanol (1 × 10 cm^3), and diethyl ether (2 × 20 cm^3), before drying *in vacuo*. The yield was 50% (0.40 g, 0.88 mmol). The material was recrystallised by slow evaporation of a saturated solution of the complex in ethyl acetate–carbon tetrachloride (1:1)

† Pencillaminate = 3-mercaptovalinate.

Supplementary data available (No. SUP 23895, 38 pp.): thermal parameters, H-atom co-ordinates, structure factors. See Instructions for Authors, *J. Chem. Soc., Dalton Trans.*, 1984, Issue 1, pp. xvii—xix.

(Found: C, 31.7; H, 5.2; Mo, 21.8; N, 6.2; S, 14.1, Calc. for $C_{12}H_{24}MoN_2O_6S_2$: C, 31.9; H, 5.3; Mo, 21.2; N, 6.2; S, 14.2%).

The corresponding (*R*)-penicillaminate complex was prepared in an identical manner (Found: C, 31.4; H, 5.3; Mo, 21.0; N, 6.0; S, 13.9%).

Instrumentation.—Ultraviolet–visible spectra were measured on a Perkin-Elmer 402 spectrometer and c.d. spectra on a Cary 61 circular dicrograph. Proton, ^{13}C, and ^{95}Mo n.m.r. spectra of solutions (typically $\geq 10^{-2}$ mol dm^{-3} in complex) at 400, 100, and 26 MHz, respectively, were recorded by Dr. B. E. Mann at the S.E.R.C. facility at the University of Sheffield; the variable-temperature ^1H n.m.r. study was accomplished using a Varian SC 300 instrument at an operating frequency of 300 MHz. Infrared spectra were recorded for Nujol mulls of the powered compounds on a Pye-Unicam SP3-300 instrument, and Raman spectra for powered solid samples on a Cary 82 instrument using excitation from the green line of an argon-ion laser (514.5 nm).

Crystal Structure Determination.—Crystals of $[MoO_2\{(S)\text{-pen-OMe}\}_2]$ suitable for structure determination by *X*-ray diffraction were obtained by slow evaporation of a solution of the compound dissolved in ethyl acetate–carbon tetrachloride (1 : 1). A crystal of dimensions *ca.* 0.30 × 0.30 × 0.12 mm [dominant faces ±(001)], sealed in a capillary tube, was examined on a Stoe-Siemens AED four-circle diffractometer, with graphite-monochromated Mo-K_α radiation (λ = 0.710 69 Å).[13] All measurements were made at room temperature. Unit-cell dimensions were refined by least-squares methods from accurate 2θ values ($20 < 2\theta < 25°$) of 32 centred reflections.

Crystal data. $C_{12}H_{24}MoN_2O_6S_2$, M = 452.4, monoclinic, space group $P2_1$, a = 11.794(2), b = 12.519(3), c = 13.040(2) Å, β = 106.32(2)°, U = 1 847.8 Å^3, Z = 4, D_c = 1.626 g cm^{-3}, $F(000)$ = 928, μ = 9.36 cm^{-1}.

Intensity data were collected in a θ–ω scan mode for reflections with $h \geq 0$ and $2\theta < 50°$; a profile-fitting procedure was used.[14] Empirical absorption corrections were applied, based on measurements of sets of equivalent reflections at various azimuthal (ψ) angles: with μ = 9.36 cm^{-1}, transmission factors ranged from 0.743 to 8.828.* 5 502 Unique reflections with $F > 4\sigma(F)$ were used for structure determination; Friedel opposites were not averaged, because anomalous-dispersion effects were exploited to verify the absolute configuration.

The molybdenum atoms of the two crystallographically independent molecules were located from a Patterson synthesis and the remaining atoms from subsequent Fourier calculations. Refinement was by a blocked-cascade least-squares method, with anisotropic thermal parameters for all non-hydrogen atoms, and a weighting scheme $w^{-1} = \sigma^2(F) + gF^2$. The quantity minimised was $\Sigma w\Delta^2$ ($\Delta = |F_o| - |F_c|$). Hydrogen atoms were constrained (C–H 0.96, N–H 0.87 Å; H–C–H = H–N–H 109.5°, all X–N–H angles equal for a $MoNH_2C$ group; C–H vector for the X_3CH tertiary C atoms lies along the sum of the C–X unit vectors) and assigned isotropic thermal parameters fixed at 1.2 times the equivalent isotropic value for the corresponding C or N atom. Final values for R ($=\Sigma|\Delta|/\Sigma|F_o|$) and for R' [$=(\Sigma w\Delta^2/\Sigma wF_o^2)^{\frac{1}{2}}$] were both 0.039. The weighting parameter g was optimised as part of the refinement; its final value was 0.000 37. All parameter shifts in the last cycles were <0.3 times the corresponding estimated standard deviations (e.s.d.s); the largest were for methyl-group rotations. A difference synthesis based on the refined parameters contained no significant features. An analysis of the variance showed no trends in the value of $V = (\Sigma w\Delta^2/\Sigma w)^{\frac{1}{2}}$ with indices, sin θ, or F_o; V, the root mean square (r.m.s.) deviation of an observation of unit weight on an absolute scale of $|F_c|$, was 1.33 e. A normal probability plot was linear, with slope 1.05.[15,16] 450 Parameters were refined.

The absolute configuration was verified by refinement of a configuration parameter η at the stage when all non-hydrogen atoms had been located.[17]† Its value was +1.22(10), clearly indicating the correct assignment. This parameter was fixed at +1 for the final refinement.

Refined co-ordinates, together with bond lengths and angles, are presented in Tables 1 and 2.

Results and Discussion

Crystal Structure.—The structures of the two independent molecules of $[MoO_2\{(S)\text{-pen-OMe}\}_2]$ are shown in Figure 1 and bond lengths and interbond angles about molybdenum are given in Table 2. Both molecules have a co-ordination sphere about molybdenum similar to that found for $[MoO_2\{(R)\text{-cys-OMe}\}_2]$ [8] and the majority of other complexes [18–21] in which a *cis*-MoO_2^{2+} moiety is ligated by two thiolate groups and two amine nitrogen atoms of bi- or quadri-dentate ligands. Thus, the penicillamine ester ligands behave as *S*,*N*-bidentate chelates with the amino-groups mutually *cis* and each *trans* to an oxygen, and the sulphur atoms mutually *trans*. In molecule 1 the Mo–O distances are 1.711(3) and 1.720(4) Å, the Mo–S distances 2.414(2) and 2.408(2) Å, and the Mo–N distances 2.340(4) and 2.347(4) Å. In molecule 2, the Mo–O distances are 1.714(4) and 1.703(3) Å, the Mo–S distances 2.404(2) and 2.403(2) Å, and the Mo–N distances 2.362(4) and 2.398(4) Å. The averages of these values [Mo–O 1.712(7), Mo–S 2.407(5), and Mo–N 2.362(26) Å] are typical of values identified previously for this type of complex.[8,18–21] Also, the Mo–O and Mo–S distances, obtained from molybdenum *K*-edge EXAFS studies of oxidised sulphite oxidase, of 1.68 and 2.41 Å, respectively,[10] are similar to the corresponding values obtained in this study.

The set of $O_2S_2N_2$ donor atoms about the molybdenum adopt a distorted-octahedral arrangement, as evidenced from the bond angles. For example, for molecules 1 and 2, respectively: O–Mo–O 107.0(2) and 107.6(2); S–Mo–S 153.4(1) and 150.8(1); N–Mo–N 83.9(1) and 81.1(1)°; ligand 'bite' angles S–Mo–N 75.9(1), 75.6(1) and 75.6(1), 75.4(1); O–Mo–S 106.7(1), 105.5(2), 89.8(2), and 89.8(1) and 105.3(2), 104.5(1), 92.5(1), and 92.1(2)°. Angular distortions, especially those for O–Mo–S and S–Mo–S, from a regular octahedral geometry have been rationalised previously [19,22] on the basis of non-bonded repulsions among the donor atoms.

The most significant difference between the two molecules is the absolute configuration about the molybdenum; in molecule 1 it is Λ, whereas in molecule 2 it is Δ.[23] The bond lengths and angles obtained (Table 2) for the penicillamine ester ligands are as expected and differ little between the two molecules, save for the Mo–S–C and Mo–N–C angles. The angles at sulphur are 107.5(2) and 107.8(2)° in the case of molecule 1 (Λ isomer), but are somewhat more acute for molecule 2 (Δ isomer), 104.1(2) and 104.2(2)°. The relative magnitudes of the Mo–N–C angles for the two molecules is the reverse of those at sulphur, the Λ isomer displaying significantly more acute angles of 110.5(3) and 111.2(3)° as compared with those for the Δ isomer of 120.4(3) and 118.6(3)°. The bond lengths around the chelate ring are fairly constant,

* Computer programs used in this study were written by G. M. Sheldrick (SHELXTL system; Göttingen) and W. Clegg (diffractometer control program) for the Data General Eclipse S250 computer.

† This refinement requires the use of complex scattering factors; these were taken from ref. 16, pp. 99 and 149.

Table 1. Fractional atomic co-ordinates ($\times 10^4$) for $[MoO_2\{(S)\text{-pen-OMe}\}_2]$

Atom	*x*	*y*	*z*	Atom	*x*	*y*	*z*
Mo(1)	9 376(1)	5 000	9 348(1)	Mo(2)	5 530(1)	3 705(1)	5 531(1)
O(1)	8 333(3)	5 382(3)	8 207(3)	O(3)	4 710(3)	2 573(3)	5 117(3)
O(2)	9 992(3)	6 149(3)	9 991(3)	O(4)	6 612(3)	3 393(3)	6 662(3)
N(1)	8 454(3)	3 341(3)	8 909(3)	N(3)	4 115(4)	4 654(4)	4 201(3)
S(1)	8 355(1)	4 720(1)	10 691(1)	S(3)	4 443(1)	4 717(1)	6 505(1)
C(11)	7 393(4)	3 534(4)	10 288(4)	C(31)	2 996(4)	4 955(4)	5 521(3)
C(12)	7 945(6)	2 587(5)	10 960(4)	C(32)	2 277(5)	3 918(4)	5 327(4)
C(13)	6 224(4)	3 819(5)	10 497(4)	C(33)	2 352(5)	5 796(5)	6 000(4)
C(14)	7 271(4)	3 347(4)	9 094(4)	C(34)	3 257(4)	5 357(4)	4 494(4)
C(15)	6 619(4)	2 315(5)	8 642(4)	C(35)	2 136(5)	5 428(4)	3 550(4)
O(11)	7 045(3)	1 546(3)	8 413(3)	O(31)	1 842(3)	4 741(3)	2 890(3)
O(12)	5 445(3)	2 440(3)	8 522(3)	O(32)	1 556(3)	6 318(3)	3 584(3)
C(16)	4 714(6)	1 557(6)	8 030(7)	C(36)	466(5)	6 453(5)	2 730(4)
N(2)	10 861(3)	3 994(4)	10 529(3)	N(4)	6 585(3)	5 353(3)	5 597(3)
S(2)	10 657(1)	4 457(1)	8 293(1)	S(4)	6 470(1)	3 557(1)	4 124(1)
C(21)	12 024(4)	3 904(4)	9 216(4)	C(41)	7 778(5)	4 437(4)	4 557(4)
C(22)	12 018(5)	2 699(4)	9 046(4)	C(42)	8 707(4)	3 936(5)	5 490(4)
C(23)	13 062(5)	4 415(5)	8 920(5)	C(43)	8 263(6)	4 531(6)	3 592(5)
C(24)	12 033(4)	4 209(4)	10 364(4)	C(44)	7 327(4)	5 504(4)	4 849(4)
C(25)	13 053(4)	3 682(5)	11 173(4)	C(45)	8 349(5)	6 282(5)	5 292(5)
O(21)	14 020(3)	4 071(3)	11 480(3)	O(41)	8 975(4)	6 603(4)	4 772(4)
O(22)	12 755(3)	2 755(3)	11 498(3)	O(42)	8 484(3)	6 516(3)	6 296(3)
C(26)	13 703(5)	2 116(5)	12 171(5)	C(46)	9 483(5)	7 156(5)	6 841(5)

Table 2. Dimensions (distances in Å, angles in degrees) with estimated standard deviations in parentheses

Molecule 1				Molecule 2			
Mo(1)–O(1)	1.711(3)	Mo(1)–O(2)	1.720(4)	Mo(2)–O(3)	1.714(4)	Mo(2)–O(4)	1.703(3)
Mo(1)–N(1)	2.340(4)	Mo(1)–N(2)	2.347(4)	Mo(2)–N(3)	2.362(4)	Mo(2)–N(4)	2.398(4)
Mo(1)–S(1)	2.414(2)	Mo(1)–S(2)	2.408(2)	Mo(2)–S(3)	2.404(2)	Mo(2)–S(4)	2.403(2)
N(1)–C(14)	1.481(7)	N(2)–C(24)	1.483(6)	N(3)–C(34)	1.470(7)	N(4)–C(44)	1.495(7)
S(1)–C(11)	1.853(5)	S(2)–C(21)	1.855(5)	S(3)–C(31)	1.848(4)	S(4)–C(41)	1.850(5)
C(11)–C(12)	1.509(8)	C(21)–C(22)	1.525(8)	C(31)–C(32)	1.532(8)	C(41)–C(42)	1.525(7)
C(11)–C(13)	1.522(8)	C(21)–C(23)	1.524(8)	C(31)–C(33)	1.531(8)	C(41)–C(43)	1.526(9)
C(11)–C(14)	1.541(7)	C(21)–C(24)	1.542(7)	C(31)–C(34)	1.541(7)	C(41)–C(44)	1.525(8)
C(14)–C(15)	1.534(7)	C(24)–C(25)	1.511(6)	C(34)–C(35)	1.535(6)	C(44)–C(45)	1.531(7)
C(15)–O(11)	1.164(7)	C(25)–O(21)	1.201(6)	C(35)–O(31)	1.198(6)	C(45)–O(41)	1.203(9)
C(15)–O(12)	1.358(6)	C(25)–O(22)	1.316(7)	C(35)–O(32)	1.314(7)	C(45)–O(42)	1.307(7)
O(12)–C(16)	1.438(8)	O(22)–C(26)	1.451(7)	O(32)–C(36)	1.455(6)	O(42)–C(46)	1.437(7)
O(1)–Mo(1)–O(2)	107.0(2)			O(3)–Mo(2)–O(4)	107.6(2)		
N(1)–Mo(1)–N(2)	83.9(1)			N(3)–Mo(2)–N(4)	81.1(1)		
S(1)–Mo(1)–S(2)	153.4(1)			S(3)–Mo(2)–S(4)	150.8(1)		
O(1)–Mo(1)–N(1)	82.2(2)	O(2)–Mo(1)–N(2)	89.6(2)	O(3)–Mo(2)–N(3)	88.0(2)	O(4)–Mo(2)–N(4)	84.9(2)
O(2)–Mo(1)–N(1)	164.9(2)	O(1)–Mo(1)–N(2)	160.5(2)	O(4)–Mo(2)–N(3)	162.6(2)	O(3)–Mo(2)–N(4)	164.4(2)
O(1)–Mo(1)–S(1)	106.7(1)	O(2)–Mo(1)–S(2)	105.5(2)	O(3)–Mo(2)–S(3)	105.3(2)	O(4)–Mo(2)–S(4)	104.5(1)
O(2)–Mo(1)–S(1)	89.8(2)	O(1)–Mo(1)–S(2)	89.8(1)	O(4)–Mo(2)–S(3)	92.5(1)	O(3)–Mo(2)–S(4)	92.1(2)
N(1)–Mo(1)–S(1)	75.9(1)	N(2)–Mo(1)–S(2)	75.6(1)	N(3)–Mo(2)–S(3)	75.6(1)	N(4)–Mo(2)–S(4)	75.4(1)
S(1)–Mo(1)–N(2)	83.0(1)	N(1)–Mo(1)–S(2)	86.2(1)	S(3)–Mo(2)–N(4)	82.9(1)	N(3)–Mo(2)–S(4)	82.0(1)
Mo(1)–N(1)–C(14)	110.5(3)	Mo(1)–N(2)–C(24)	111.2(3)	Mo(2)–N(3)–C(34)	120.4(3)	Mo(2)–N(4)–C(44)	118.6(3)
Mo(1)–S(1)–C(11)	107.5(2)	Mo(1)–S(2)–C(21)	107.8(2)	Mo(2)–S(3)–C(31)	104.1(2)	Mo(2)–S(4)–C(41)	104.2(2)
S(1)–C(11)–C(12)	109.6(3)	S(2)–C(21)–C(22)	107.9(3)	S(3)–C(31)–C(32)	109.8(3)	S(4)–C(41)–C(42)	110.5(4)
S(1)–C(11)–C(13)	105.9(4)	S(2)–C(21)–C(23)	107.0(3)	S(3)–C(31)–C(33)	107.1(3)	S(4)–C(41)–C(43)	105.6(3)
C(12)–C(11)–C(13)	110.2(5)	C(22)–C(21)–C(23)	110.5(5)	C(32)–C(31)–C(33)	109.6(4)	C(42)–C(41)–C(43)	109.7(5)
S(1)–C(11)–C(14)	106.5(4)	S(2)–C(21)–C(24)	107.8(3)	S(3)–C(31)–C(34)	106.5(3)	S(4)–C(41)–C(44)	106.2(4)
C(12)–C(11)–C(14)	111.8(4)	C(22)–C(21)–C(24)	112.6(4)	C(32)–C(31)–C(34)	111.7(4)	C(42)–C(41)–C(44)	112.6(4)
C(13)–C(11)–C(14)	112.6(4)	C(23)–C(21)–C(24)	110.8(4)	C(33)–C(31)–C(34)	111.9(4)	C(43)–C(41)–C(44)	112.1(5)
N(1)–C(14)–C(11)	109.9(3)	N(2)–C(24)–C(21)	110.1(3)	N(3)–C(34)–C(31)	110.5(4)	N(4)–C(44)–C(41)	111.2(4)
N(1)–C(14)–C(15)	109.1(4)	N(2)–C(24)–C(25)	114.3(4)	N(3)–C(34)–C(35)	109.1(4)	N(4)–C(44)–C(45)	112.2(4)
C(11)–C(14)–C(15)	114.2(4)	C(21)–C(24)–C(25)	110.9(4)	C(31)–C(34)–C(35)	112.2(4)	C(41)–C(44)–C(45)	111.0(4)
C(14)–C(15)–O(11)	126.1(5)	C(24)–C(25)–O(21)	123.4(5)	C(34)–C(35)–O(31)	123.0(5)	C(44)–C(45)–O(41)	122.9(5)
C(14)–C(15)–O(12)	109.4(5)	C(24)–C(25)–O(22)	112.2(4)	C(34)–C(35)–O(32)	111.2(4)	C(44)–C(45)–O(42)	112.4(5)
O(11)–C(15)–O(12)	124.5(5)	O(21)–C(25)–O(22)	124.4(4)	O(31)–C(35)–O(32)	125.8(4)	O(41)–C(45)–O(42)	124.6(5)
C(15)–O(12)–C(16)	115.2(5)	C(25)–O(22)–C(26)	116.7(4)	C(35)–O(32)–C(36)	115.4(4)	C(45)–O(42)–C(46)	118.2(5)

Table 3. Torsion angles (°) around the *S,N*-chelate rings in *cis*-[MoO{(*S*)-pen-OMe}$_2$]

Angle *	Molecule 1, Λ diastereoisomer		Molecule 2, Δ diastereoisomer	
	Ligand 1	Ligand 2	Ligand 3	Ligand 4
Mo–S(X)–C(X1)–C(X4)	−17.3	−13.2	−47.9	−50.3
S(X)–C(X1)–C(X4)–N(X)	50.3	46.2	49.4	50.7
C(X1)–C(X4)–N(X)–Mo	−62.5	−60.7	−28.8	−28.2
C(X4)–N(X)–Mo–S(X)	37.9	39.0	−1.2	−3.0
N(X)–Mo–S(X)–C(X1)	−9.2	−11.8	24.6	26.3
H(X4)–C(X4)–N(X)–H(XA)	174.3	178.4	−149.8	−149.3
H(X4)–C(X4)–N(X)–H(XB)	−66.1	−62.2	−32.9	−31.8

* See Figure 1 for atom labelling.

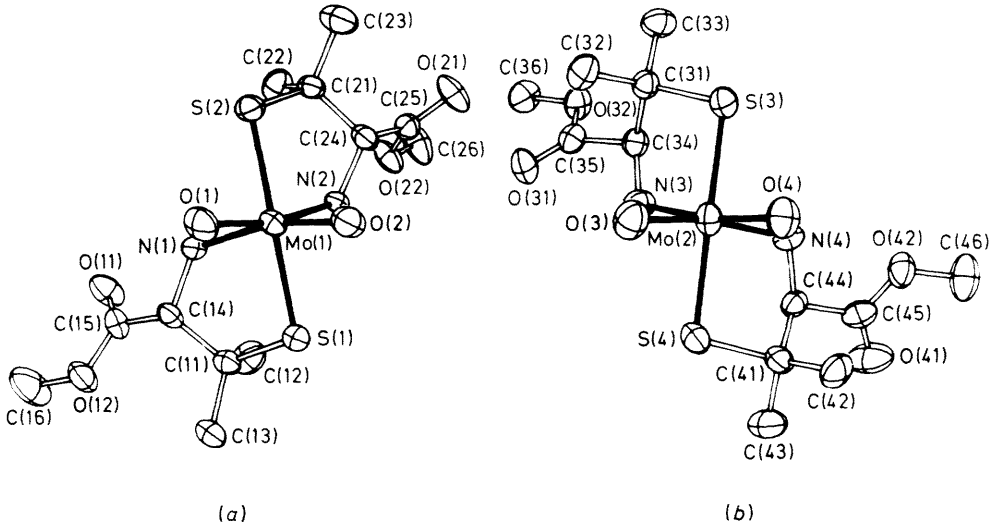

Figure 1. Structures of (*a*) Λ- and (*b*) Δ-*cis*-[MoO$_2$\{(*S*)-pen-OMe\}$_2$], molecules 1 and 2, respectively

with average values of 1.851(9) Å for the S–C bond, 1.482(20) Å for the N–C bond, and 1.534(17) Å for the intervening C–C bond. Torsion angles, describing the conformations of the *S,N*-chelate rings, are listed in Table 3. In each case, the conformation of the ring is δ, positioning the CO_2Me substituent equatorial to the chelate ring, but the detailed conformation is significantly different in the two molecules. The torsion angles subtended by S(X) and N(X) about the C(X1)–C(X4) bonds are all *ca.* 50°, but differences of up to 40° are observed between other analogous torsion angles of the Λ and Δ isomers.

Hydrogen-atom positions were included in the final refinement of the structure, subject to constraints (see Experimental section), and torsion angles between the α-proton [H(X4)] and the two amine protons [H(XA) and H(XB)] are included in Table 3. For molecule 1 the H(X4)–C(X4)–N(X)–H(XA) torsion angles are 174 (X = 1) and 178° (X = 2) and H(X4)–C(X4)–N(X)–H(XB) are −66 (X = 1) and −62° (X = 2) for ligands 1 and 2, respectively. In the case of molecule 2, the torsion angles to H(XA) are 150 (X = 3) and 149° (X = 4) and to H(XB) are −33 (X = 3) and −32° (X = 4) for ligands 3 and 4, respectively.

Vibrational Spectroscopy.—*cis*-Dioxomolybdenum(VI) complexes generally give rise to two strong ν(Mo–O$_t$) vibrations close to 900 cm^{-1}, both of these modes being strongly i.r. and Raman active.[1] For sulphite oxidase the molybdenum(VI) centre appears to manifest these vibrations at 924 and 900 cm^{-1} in the Raman.[9]

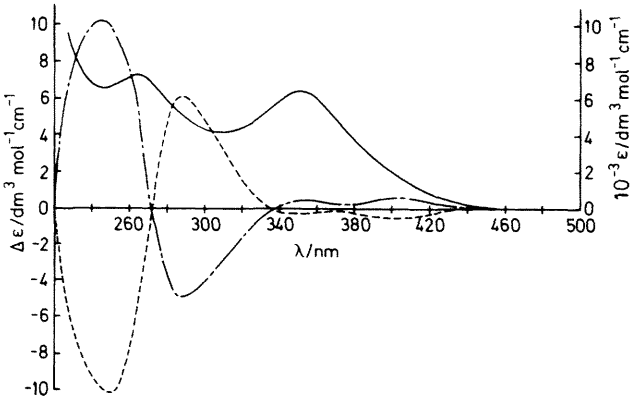

Figure 2. Electronic absorption spectrum of *cis*-[MoO$_2$\{(*S*)-pen-OMe\}$_2$] (———) and c.d. spectra of *cis*-[MoO\{(*S*)-pen-OMe\}$_2$] (— — —) and *cis*-[MoO$_2$\{(*R*)-pen-OMe\}$_2$] (– – –) recorded in MeCN solution

In the i.r. spectrum of [MoO$_2$\{(*S*)-pen-OMe\}$_2$] these two bands are resolved as a pair of doublets at 918 and 913 cm^{-1} and at 878 and 875 cm^{-1}. This presumably arises from the slightly different ν(Mo–O$_t$) frequencies of the Λ and Δ diastereoisomers of the complex. It has not proved possible to effect such resolution of the Raman spectrum, which displays two bands centred at 918 and 878 cm^{-1}.

Table 4. Electronic absorption and c.d. spectra [a] of penicillaminate ester complexes of *cis*-dioxomolybdenum(VI)

Complex	Solvent	Spectrum	λ/nm ($10^{-3}\varepsilon$ or $\Delta\varepsilon$/dm^3 mol^{-1} cm^{-1})			
$[MoO_2\{(S)\text{-pen-OMe}\}_2]$	MeCN	Absorption	264 (7.24)		352 (6.45)	
	MeCN	c.d.	245 (+10.2)	288 (−4.9)	350 (+0.5)	400 (+0.7)
	MeOH	c.d.	234 (+8.1)	282 (−4.8)	347 (+0.3)	400 (+0.7)
	$HCONMe_2$	c.d.	*b*	288 (−12.0)	346 (+0.3)	393 (+2.0)
	Me_2SO	c.d.	*b*	292 (−8.5)	347 (+0.3)	398 (+1.6)
$[MoO_2\{(R)\text{-pen-OMe}\}_2]$	MeCN	Absorption	236 (7.68)		352 (7.11)	
	MeCN	c.d.	250 (−10.1)	288 (+6.1)	352 (−0.3)	405 (−0.5)

[a] Recorded on solutions 10^{-3}—10^{-4} mol dm^{-3} in complex, in 1-cm pathlength silica cells. [b] Obscured by solvent absorption.

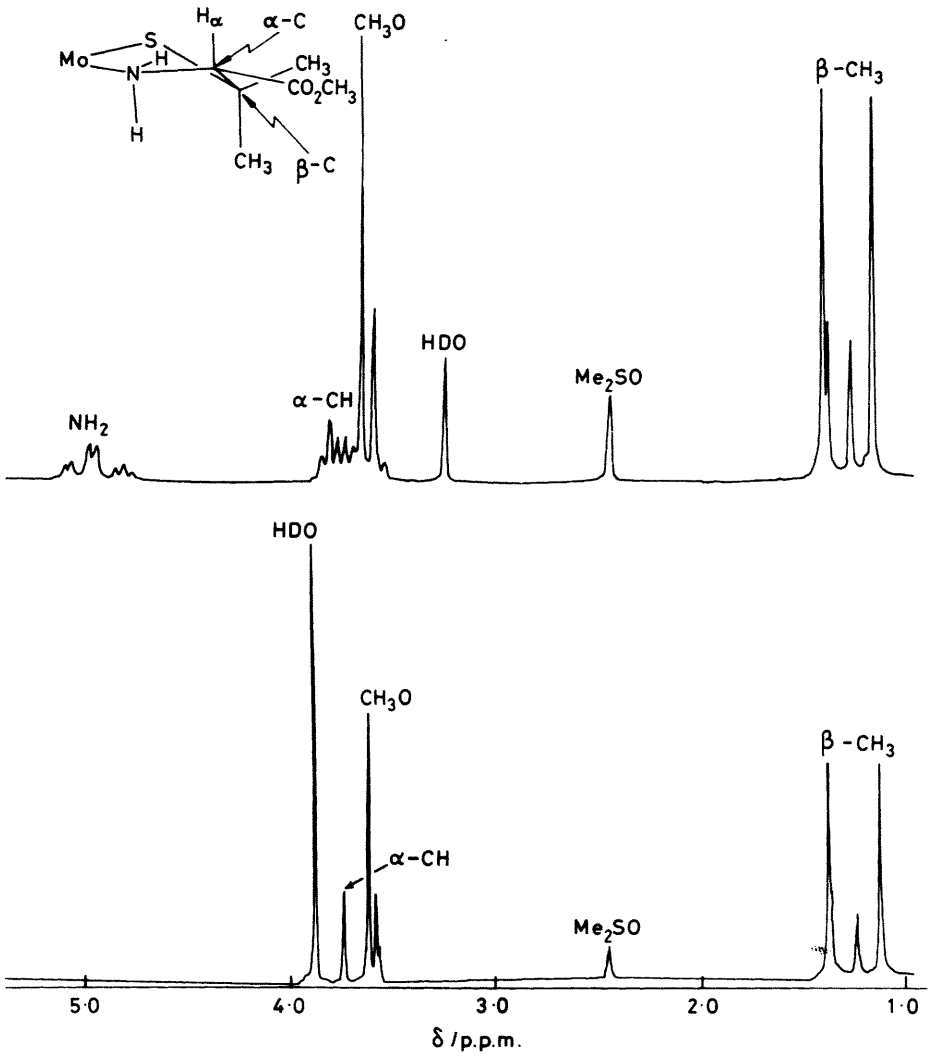

Figure 3. 300-MHz ^{1}H n.m.r. spectrum of *cis*-$[MoO_2\{(R)\text{-pen-OMe}\}_2]$ in $(CD_3)_2SO$ at 24 °C (top) and in $[^2H_6]$dimethyl sulphoxide–water at 24 °C (bottom). Pulse angle 70°, pulse repetition 3 s, digital resolution 0.6 Hz, line broadening 0.5 Hz (exponential multiplication)

Electronic and C.D. Spectra.—The electronic spectra of *cis*-dioxomolybdenum(VI) complexes typically exhibit one or two absorption maxima in the 380—250 nm region [1,8,24-26] and it has been noted [7,8,27] that complexes of this moiety with chiral ligands show strong optical activity. The optical properties of *cis*-$[MoO_2\{(S)\text{-pen-OMe}\}_2]$ (Table 4) are a further demonstration of these general statements; spectra are plotted in Figure 2, which also indicates that the c.d. spectra of the *R*- and the *S*-penicillamine ester complexes have the expected catoptric relationship.

The four Cotton effects at *ca.* 400, 350, 290, and 240 nm are similar to those recorded for *cis*-$[MoO_2\{(R)\text{-cys-OMe}\}_2]$.[7,8] However a comparison of the profiles for these MoO_2^{2+} complexes of the two (*R*)-ligands reveals that Δε at *ca.* 400, 290, and 240 nm (but not at *ca.* 350 nm, the weakest band for *cis*-$[MoO_2\{(R)\text{-pen-OMe}\}_2]$) has the opposite sign from one complex to the other. Proton, ^{13}C, and ^{95}Mo n.m.r. spectra are consistent with both *cis*-$[MoO_2\{(R)\text{-cys-OMe}\}_2]$ [7,8] and *cis*-$[MoO_2\{(R)\text{-pen-OMe}\}_2]$ (see below) existing as two diastereoisomeric molecules in solution in unequal concentrations.

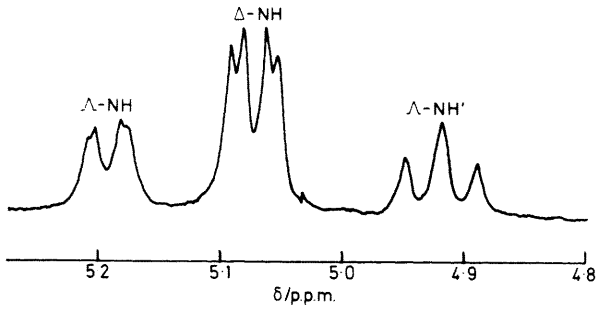

Figure 4. 400-MHz ^{1}H n.m.r. spectrum of *cis*-[MoO_2(*R*)-pen-OMe}$_2$] in $(CD_3)_2SO$ at 24 °C in the region 4.8—5.3 p.p.m. Pulse angle 25°, pulse repetition 3.3 s, digital resolution 0.3 Hz, no enhancement or line broadening

The reversal of the sign of Δε from *cis*-[MoO_2{(*R*)-cys-OMe}$_2$] to *cis*-[MoO_2{(*R*)-pen-OMe}$_2$] is taken to indicate that the major solution species of each compound has the opposite configuration at molybdenum. The complex *cis*-[MoO_2{(*R*)-cys-OMe}$_2$] exists in solution as two species in a ratio of *ca.* 5 : 1 and the Λ diastereoisomer has been argued [7,8] to predominate since this is present *exclusively* in the crystalline state. Therefore, solutions of *cis*-[MoO_2{(*R*)-pen-OMe}$_2$] are deduced to contain the Δ and Λ diastereoisomers in a 2 : 1 ratio and *cis*-[MoO_2{(*S*)-pen-OMe}$_2$] to dissolve to yield the Λ and Δ isomers in 2 : 1 relative concentrations. Furthermore, the absolute magnitude of each of the Δε values for *cis*-[MoO_2{(*R*)-pen-OMe}$_2$] is smaller than the corresponding values of *cis*-[MoO_2{(*R*)-cys-OMe}$_2$]. This observation is consistent with the n.m.r. results, referred to above, which show a more even distribution between the two chiralities at molybdenum for *cis*-[MoO_2{(*R*)-pen-OMe}$_2$] (Δ : Λ is *ca.* 2 : 1) than for *cis*-[MoO_2{(*R*)-cys-OMe}$_2$] (Δ : Λ is *ca.* 1 : 5).

The magnitude of the Δε values at *ca.* 400 and 290 nm manifests a significant solvent dependence, the reasons for which are unclear. As observed for *cis*-[MoO_2{(*R*)-cys-OMe}$_2$],[7,8] the c.d. spectra of the penicillamine ester complexes of MoO_2^{2+} (Figure 2) resolve each of the maxima in the corresponding absorption spectrum into two components. The assignments of these electronic transitions, although clearly of a ligand-to-metal charge-transfer nature for this d^0 centre, are uncertain. Oxygen-to-molybdenum charge transfer within a *cis*-MoO_2^{2+} group has been suggested [24,25] to give rise to an absorption at *ca.* 300 nm; the c.d. feature(s) at *ca.* 290 (and 240) nm could be consistent with their view. Sulphur-to-molybdenum charge-transfer transitions would also be expected to occur at a relatively low energy and, in the case of *cis*-[MoO_2-$(S_2CNEt_2)_2$], these were considered to be the cause of the absorption at 379 nm. A similar assignment may be appropriate to either one or both of the electronic absorptions at *ca.* 350 and 400 nm. However, as noted earlier, the sign of Δε for the band at 400 nm reverses between *cis*-[MoO_2{(*R*)-cys-OMe}$_2$] and *cis*-[MoO_2{(*R*)-pen-OMe}$_2$] but the sign of the band at 350 nm does not. This may imply some difference in the origin of these two transitions.

N.M.R. Spectra.—^{1}H *Spectra.* The 300-MHz ^{1}H n.m.r. spectrum of *cis*-[MoO_2{(*R*)-pen-OMe}$_2$] in $(CD_3)_2SO$ at 24 °C is shown in Figure 3 and, as expected, the corresponding spectrum of *cis*-[MoO_2{(*S*)-pen-OMe}$_2$] is identical. The interpretation of this spectrum is complicated. (*i*) By the superposition of signals due to two solution species, present in the ratio of *ca.* 2 : 1, in view of the crystallographic results and consistent with these n.m.r. data, these species are presumed to be the Λ and Δ diastereoisomers. Arguments based

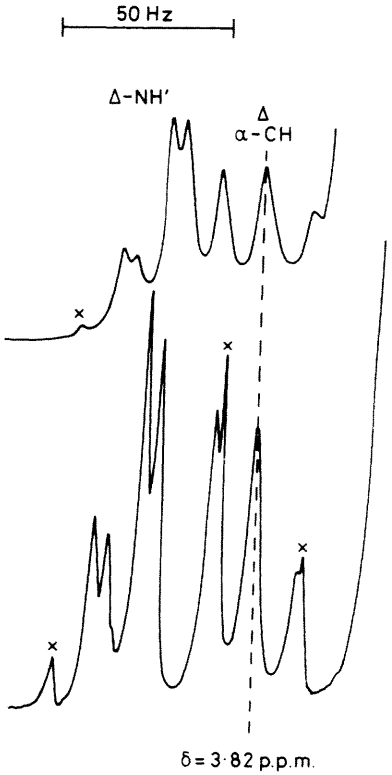

Figure 5. Portions of the ^{1}H n.m.r. spectra of *cis*-[MoO_2(*R*)-pen-OMe}$_2$] in $(CD_3)_2SO$ at 24 °C, recorded at 300 (upper) and 400 MHz (lower); the spectra are plotted on the same frequency scale and are aligned at δ = 3.82 p.p.m. (spinning side bands denoted by X). For recording parameters, see Figures 3 and 4

on comparison of the c.d. spectra of *cis*-[MoO_2{(*R*)-pen-OMe}$_2$] and *cis*-[MoO_2{(*R*)-cys-OMe}$_2$] presented above led to the conclusion that for solutions of *cis*-[MoO_2{(*R*)-pen-OMe}$_2$] the Δ diastereoisomer predominates, thus for *cis*-[MoO_2{(*S*)-pen-OMe}$_2$] the Λ diastereoisomer is considered to be the principal species. (*ii*) By two complicated ABX patterns centred at *ca.* 5.1 and 3.9 p.p.m., which are assigned to the Mo–NH_2–C_αH fragments of the diastereoisomers. This region of the spectrum is greatly simplified by the addition of D_2O to the solution (Figure 3). The amine protons exchange rapidly with D_2O to produce a prominant HOD resonance at *ca.* 4.0 p.p.m., leaving the H_α signals as unsplit singlets. This proton exchange, although not unexpected, is of interest in respect of the proton exchange observed by e.s.r. spectroscopy [28] for the molybdenum(v) centres of the oxo-enzymes. Unfortunately, the rate of this amine-proton exchange with D_2O is too rapid for monitoring by conventional n.m.r. techniques and an upper limit of $t_{\frac{1}{2}} < 30$ s ($k > 0.02$ s^{-1}) is suggested for this process.

The assignment of the majority of resonances in the ^{1}H n.m.r. spectrum of *cis*-[MoO_2{(*R*)-pen-OMe}$_2$] is as follows. The major diastereoisomer (Δ) is considered to have the $C_\beta(CH_3)_2$ resonances at 1.45 and 1.19 p.p.m., the methyl ester and the CH_α resonances at 3.74 and 3.82 p.p.m., respectively. For the minor diastereoisomer (Λ), the $C_\beta(CH_3)_2$ resonances are observed at 1.41 and 1.30 p.p.m., and the CH_α and CO_2CH_3 resonances at 3.64 and 3.67 p.p.m., respectively.

The interpretation of the unexchanged spectrum in the region 3.8—5.3 p.p.m. requires further comment. The three profiles centred at 5.19, 5.07, and 4.92 p.p.m. (Figure 4), with relative integrations of 1 : 2 : 1, are assigned to amino-protons

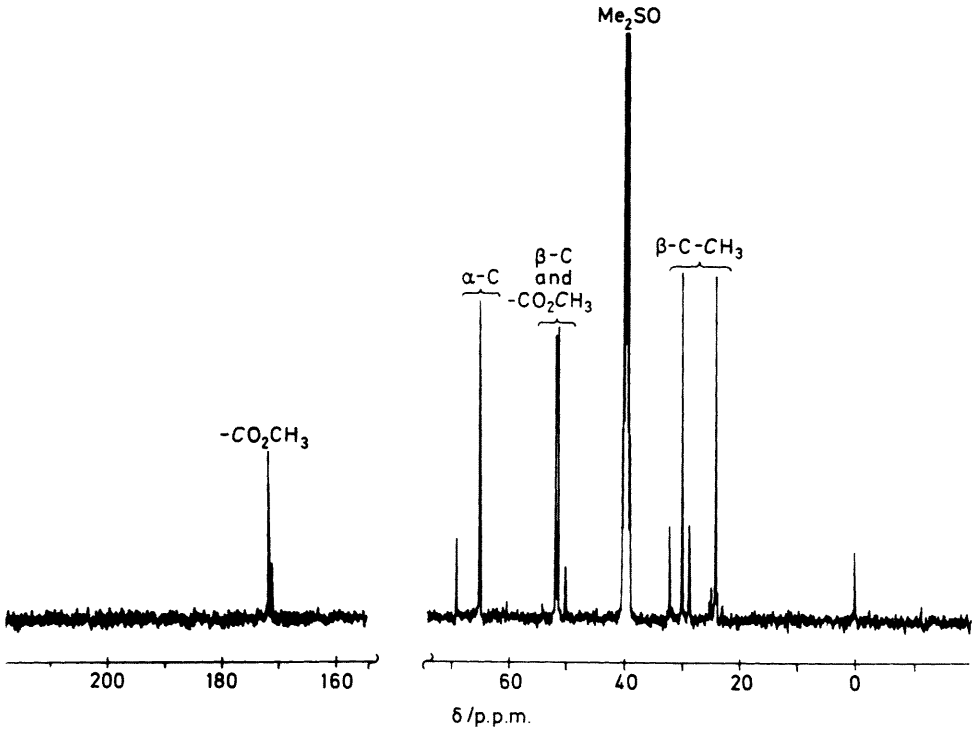

Figure 6. 100-MHz, Broad-band proton-decoupled, ^{13}C n.m.r. spectrum of *cis*-[MoO_2{(*R*)-pen-OMe}$_2$] in $(CD_3)_2SO$ at 24 °C. Pulse angle 25°, digital resolution 1.5 Hz, pulse repetition 0.65 s, line broadening 3 Hz (exponential multiplication)

of the minor (Λ-NH), major (Δ-NH), and minor (Λ-NH′) diastereoisomers, respectively. The other amine-proton resonance of the major isomer (Δ-NH′) is considered to be located in the 3.5—4.0 p.p.m. region. Comparison of the 300- and 400-MHz ^1H n.m.r. spectra of *cis*-[MoO_2{(*R*)-pen-OMe}$_2$], in $(CD_3)_2SO$ at 24 °C (Figure 5), demonstrates that there are two different proton resonances in this region. The separations (in Hz) of the four lines in the low-field region of this spectrum are independent of the operating frequency of the spectrometer, as are the separations of the three lines in the high-field region. However, the separation between these two sets of peaks shows a marked dependence on the operating frequency and thus corresponds to a chemical shift difference between two types of proton environment. Decoupling of both of these resonances collapses the resonance at 5.07 p.p.m. to a singlet, without affecting the resonances at 4.92 and 5.19 p.p.m. Decoupling of the resonance at 5.07 p.p.m. collapses the resonances in the 3.8 p.p.m. region to an AB quartet interpreted [29] as involving chemical shifts of 3.91 and 3.82 p.p.m. The latter is the same as the chemical shift assigned earlier to CH_α of the major diastereoisomer in the D_2O-exchanged spectrum, thus the former is assigned to the other amino-proton (Δ-NH′) resonance of this isomer. The coupling constants for this system are $^2J(NH,NH') = 3.8$, $^3J(NH,CH_\alpha) = 12.5$, and $^3J(NH',CH_\alpha) = 12.5$ Hz and, since both of the amine protons experience the same vicinal coupling constants to CH_α, the Δ-CH_α resonance appears as a triplet (Figure 5). The two different coupling constants experienced by each amine proton result in a four-line pattern for each (Figures 4 and 5), although we note that $^2J(NH,NH')$ is unexpectedly small. The couplings of the amino-proton resonances observed for the minor diastereoisomer (Λ) show some differences to those of the major diastereoisomer, presumably reflecting different conformations for the chelate rings of the two molecules; $^2J(NH,NH') = 10.0$, $^3J(NH,CH_\alpha) = 2.0$, and $^3J(NH,CH_\alpha) = 14.0$ Hz, the similarity between the first and last values resulting in the Λ-NH′ resonance being manifest as a triplet (Figure 4).

Assuming that the approximation (1), which relates [29] the

$$^3J \approx 10 \cos^2\theta \qquad (1)$$

vicinal coupling constant to the torsion angle θ subtended by two protons about an intervening C–C or C–N bond, holds for these molecules, the ^3J values observed imply that the C–N portions of the chelate rings of each diastereoisomer have significantly different conformations in solution, as compared to the crystalline state. Furthermore, the crystallographic data do not provide a clear indication as to why one, and only one, of the amine protons (Δ-NH′) is significantly shifted upfield (δ = 3.91 p.p.m.); in this respect, we have considered hydrogen-bonding effects and the possible diamagnetic anisotropy induced by the electron density in the Mo=O bonds. A similar observation and comment has been made [8] for *cis*-[MoO_2{(*R*)-cys-OMe}$_2$], for which a resonance at 4.16 p.p.m. was attributed to an amino-proton of the minor solution constituent (Δ). However, we note that the interpretations of the c.d. and ^1H n.m.r. spectra presented above are consistent, in that this unusual amino-proton resonance occurs for *both* the Δ isomers of these (*R*)-ligand complexes.

^{13}C *Spectra.* The 100-MHz ^{13}C n.m.r. spectrum of *cis*-[MoO_2{(*R*)-pen-OMe}$_2$] in $(CD_3)_2SO$ at 24 °C is shown in Figure 6 and the resonance positions are summarised in Table 5. Although each penicillaminate methyl ester ligand contains six carbon environments, this spectrum manifests twice as many resonances, consistent with the presence of two solution species and the integrations indicate a relative population of *ca.* 2 : 1. Thus, these details are in accord with the ^1H n.m.r. spectra and the same labelling of the major (Δ) and minor (Λ) solution species has been adopted in the assign-

Table 5. ^{13}C N.m.r. spectra [a] of (*R*)-penicillamine methyl ester and its *cis*-MoO_2^{2+} diastereoisomers

Derivative	C_α	C_β	C_β–CH_3		CO_2CH_3	CO_2CH_3
pen-OMe·HCl [b]	63.45	44.47	30.44	28.52	169.04	54.51
Δ-*cis*-[MoO_2{(*R*)-pen-OMe}$_2$] [c]	65.24	51.94	29.94	24.15	171.89	51.41
Λ-*cis*-[MoO_2{(*R*)-pen-OMe}$_2$] [c]	69.26	51.68	32.08	28.68	171.30	50.11

[a] Chemical shifts in p.p.m. downfield of $SiMe_4$. [b] Recorded at 20 MHz for a D_2O solution at 24 °C. [c] Recorded at 100 MHz for a $(CD_3)_2SO$ solution at 24 °C.

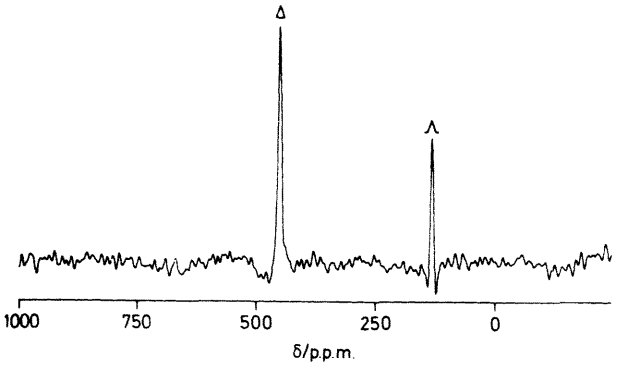

Figure 7. 26-MHz ^{95}Mo n.m.r. spectrum of *cis*-[MoO_2{(*R*)-pen-OMe}$_2$] in dimethylformamide–[$^2H_6$]dimethyl sulphoxide (4 : 1 by volume) at 45 °C. Pulse width = 60°, digital resolution 15 Hz, pulse repetition 0.065 s, with no enhancement or broadening

ment of the ^{13}C resonances in Table 5. These assignments have been aided by the 20-MHz ^{13}C spectrum of (*R*)-penicillamine methyl ester hydrochloride in D_2O at 24 °C and previously reported [30] ^{13}C n.m.r. spectra. The ^{13}C n.m.r. spectrum of *cis*-[MoO_2{(*S*)-pen-OMe}$_2$] is identical to that of *cis*-[MoO_2{(*R*)-pen-OMe}$_2$] and in this case the two diastereoisomers are considered to be present with Λ : Δ of *ca.* 2 : 1.

^{95}Mo *Spectrum.* The 26-MHz ^{95}Mo n.m.r. spectrum of *cis*-[MoO_2{(*R*)-pen-OMe}$_2$] in dimethylformamide–[$^2H_6$]-dimethyl sulphoxide (4 : 1 by volume) at 45 °C is reproduced in Figure 7. Two well separated resonances are observed at 450.7 and 131.3 p.p.m. (downfield of aqueous $[MoO_4]^{2-}$). These data are consistent with the above discussion, the downfield and upfield resonances being assigned to the Δ and Λ diastereoisomers, respectively, and the resonance positions being in the region reported previously [8,31] for *cis*-MoO_2^{2+} complexes with sulphur donor ligands. However, the considerable difference in the resonance positions (319.4 p.p.m.) is remarkable, especially since the ^{95}Mo chemical shifts of the diastereoisomers of *cis*-[MoO_2{(*R*)-cys-OMe}$_2$] differ by only 27.7 p.p.m.[8]

Variable-temperature ^1H *n.m.r. study.* 300-MHz Proton n.m.r. spectra of *cis*-[MoO_2{(*S*)-pen-OMe}$_2$] in $(CD_3)_2SO$ solution were collected over as wide a temperature range as possible, namely 24—112 °C, the upper limit being determined by the onset of sample decomposition. As the temperature of the sample was increased, coalescence of the two sets of resonances was observed, consistent with the optical isomerisation (2). The most convenient region of the ^1H n.m.r. spectrum for lineshape analysis was the $C_\beta(CH_3)_2$ region (*ca.* δ = 1.5 p.p.m.), with special consideration being given to the coalescence of the upfield pair of singlets (Figure 8). The

$$\Delta\text{-}cis\text{-}[MoO_2\{(S)\text{-pen-OMe}\}_2] \underset{k_{-1}}{\overset{k_1}{\rightleftharpoons}} \Lambda\text{-}cis\text{-}[MoO_2\{(S)\text{-pen-OMe}\}_2] \quad (2)$$

observed, digitised, spectral data were fitted to an expression [32,*] for the lineshape as a function of frequency for the various temperatures employed, using a non-linear regression (curve-fitting) routine.[33] The data obtained are summarised in Table 6; the observed spectra are compared with the profiles calculated [34] from these parameters in Figure 8. Eyring [35] plots constructed from the data of Table 6 gave activation parameters (and their 95% confidence limits based on a least-squares analysis) for the Δ ⟶ Λ interconversion of $\Delta H^\ddagger$ = 41.8 ± 3.3 kJ mol^{-1}, $\Delta S^\ddagger$ = −108 ± 9 J K^{-1} mol^{-1}, and $\Delta G^\ddagger$ = 74.0 ± 6.0 kJ mol^{-1} and for the reverse reaction of $\Delta H^\ddagger$ = 43.6 ± 6.0 kJ mol^{-1}, $\Delta S^\ddagger$ = −110 ± 17 J K^{-1} mol^{-1}, and $\Delta G_{298}^\ddagger$ = 76.4 ± 11.1 kJ mol^{-1}. Comparison of these values yields overall thermodynamic parameters for reaction (2) of $\Delta H^\ominus \approx -1.8$ kJ mol^{-1}, $\Delta S^\ominus \approx 2$ J K^{-1} mol^{-1}, and $\Delta G_{298}^\ominus \approx 2.4$ kJ mol^{-1}; at 298 K, the equilibrium constant, $K = [\Lambda]/[\Delta]$, is calculated to be *ca.* 2.6, consistent with the value of *ca.* 2.0 obtained from integrations of the ^1H n.m.r. data obtained at this temperature.

The rate of interconversion of the Δ and Λ diastereoisomers of *cis*-[MoO_2{(*S*)-pen-OMe}$_2$], if generally applicable to [$MoO_2(L\text{–}L)_2$] complexes, indicates that (since $t_{\frac{1}{2}} \approx 2$ s) optical resolution of these prochiral complexes is unlikely to be achieved. The possible mechanisms for the inversion of configuration about chiral metal atoms, particularly for tris(bidentate chelate) complexes, have received considerable attention.[36] The postulated mechanisms may be broadly

Table 6. Interpretation of the variable-temperature, 300-MHz, ^1H n.m.r. data obtained for *cis*-[MoO_2{(*S*)-pen-OMe}$_2$] in $(CD_3)_2SO$

T/K	X_Λ [a]	$k_{obs.}$/s^{-1}	k_1 [b]/s^{-1}	k_{-1} [c]/s^{-1}	Quality of fit [d]
297 ± 2	0.711	1.75 ± 0.06	1.24	0.51	50
332 ± 3	0.709	5.94 ± 1.10	4.21	1.73	347
340 ± 3	0.717	8.46 ± 1.20	6.07	2.39	277
346 ± 3	0.719	10.62 ± 1.10	7.63	2.99	141
362 ± 3	0.687	26.49 ± 2.80	18.20	8.29	203
374 ± 5	0.684	36.94 ± 4.20	25.25	11.69	163
385 ± 5	0.712	53.12 ± 10.0	37.79	15.33	70

[a] Mole fraction of Λ-*cis*-[MoO_2{(*S*)-pen-OMe}$_2$]. [b] Δ → Λ. [c] Λ → Δ. [d] Residual sum of the squares.

* For a two-site exchange (A ⇌ B), the n.m.r. lineshape, $S(\omega)$, as a function of the frequency, ω in Hz, may be expressed as the real part of expression (i) where $M_{11} = -i(\omega_A - \omega) - (1/T_{2A}) - (X_B/X_A\tau_B)$, $M_{12} = 1/\tau_B$, $M_{21} = (X_B/X_A\tau_B)$, and $M_{22} = -i(\omega_B - \omega) - (1/T_{2B}) - (1/\tau_B)$; X_A and X_B are the mole fractions of the two exchanging sites, τ_A and τ_B their mean lifetimes, T_{2A} and T_{2B} their spin–spin relaxation times, ω_A and ω_B are the frequencies of the two resonances in the absence of exchange, and ω is the midpoint of the spectrum.

$$S(\omega) = [X_A \quad X_B]\begin{bmatrix} M_{11} & M_{21} \\ M_{12} & M_{22} \end{bmatrix}^{-1}\begin{bmatrix} 1 \\ 1 \end{bmatrix} \quad \text{(i)}$$

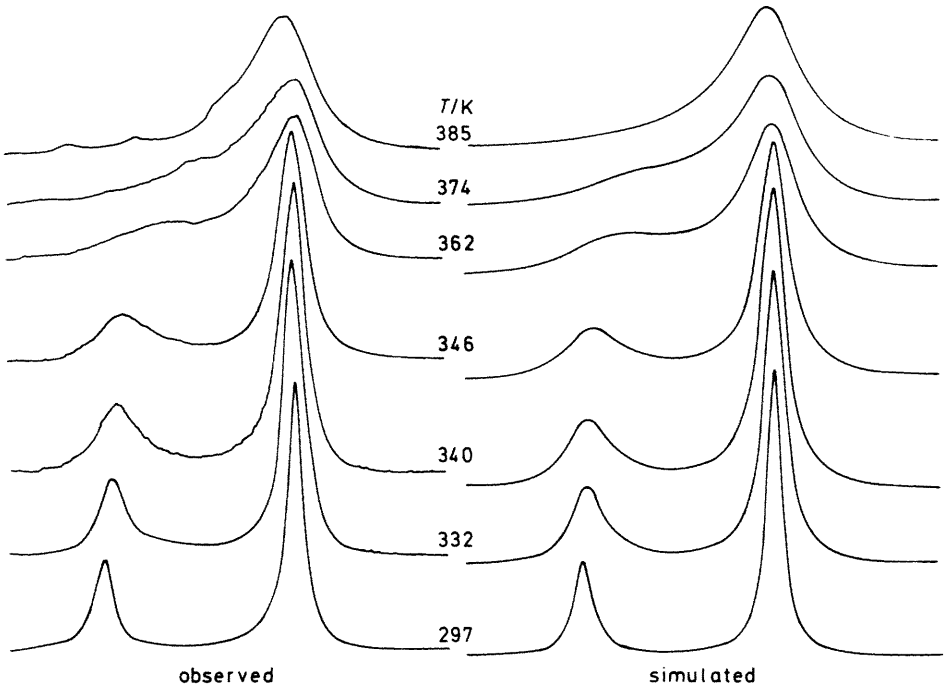

Figure 8. Comparison of the profiles observed and calculated [34] from the parameters of Table 6, for the coalescence of the high-field $C_\beta(CH_3)_2$ 300-MHz ^1H resonances of Λ- and Δ-*cis*-[MoO_2{(*S*)-pen-OMe}$_2$] in $(CD_3)_2SO$

classified as (*i*) intermolecular or (*ii*) intramolecular. The former can be excluded because the temperature dependence of the ^1H n.m.r. spectrum of *cis*-[MoO_2{(*S*)-pen-OMe}$_2$] is unaffected by a change in the concentration of this complex. Intramolecular processes, leading to inversion of configuration, may be further classified as: (*iia*) those involving rupture of one end of a chelate ring from the metal, followed by rotation of the subsequent intermediate prior to ring closure; and (*iib*) those involving twisting of the chelate rings past one another, but involving no bond rupture. A consideration of the latter mechanism, in respect of Λ-[MoO_2{(*S*)-pen-OMe}$_2$], has shown that all conceivable twists which result in an inversion of configuration about molybdenum result also in geometrical isomerisation, changing the *cis–trans* relationships of the various donor atoms. Such geometrical isomerism is not supported by the ^1H, ^{13}C, and ^{95}Mo n.m.r. spectra, since only two species (the Λ and Δ isomers) are observed in solution. Therefore, a twisting mechanism can be ruled out in the present case.

Mechanism (*iia*) is an attractive one for [$MoO_2(L{-}L)_2$] complexes, since terminal oxo-ligands are known to exert a strong *trans* effect; thus relatively long Mo–N bonds are observed crystallographically for *cis*-[MoO_2{(*S*)-pen-OMe}$_2$]. Therefore, it seems reasonable to suggest that these Mo–N bonds are susceptible to cleavage. Rotation of the ligand atoms of the intermediate so produced, followed by ring closure, would effect the inversion of configuration at the molybdenum *without* geometric isomerisation. The essence of this mechanism is summarised in the Scheme.

A mechanism involving dissociation of the ligand (Ph_3PO) *trans* to a terminal oxo-group has been described for the S_N1 displacement of Ph_3PO from [$MoOCl_3(Ph_3PO)_2$] by halide (Cl^- or Br^-).[37] The activation parameters obtained for these displacements bear a striking resemblance to those measured for inversion of *cis*-[MoO_2{(*S*)-pen-OMe}$_2$]: for displacement by chloride, $\Delta H^\ddagger = 44.4 \pm 3$ kJ mol^{-1}, $\Delta S^\ddagger = -64 \pm 12$ J K^{-1} mol^{-1}; for displacement by bromide, $\Delta H^\ddagger = 47.7 \pm 1$ kJ

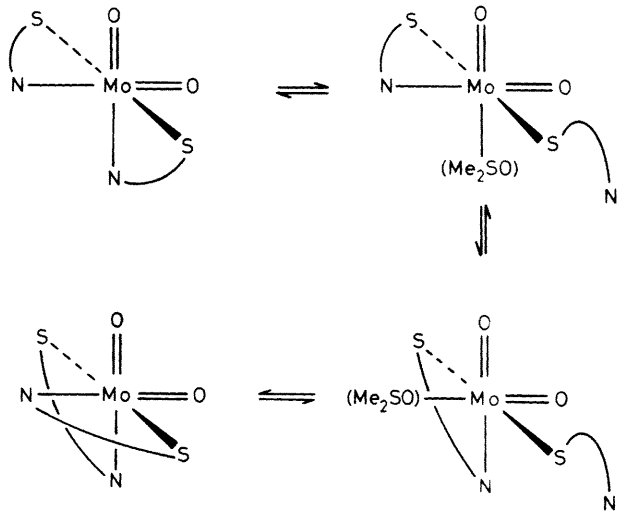

Scheme. Interconversion of Δ- and Λ-diastereoisomers of *cis*-[MoO_2{(*S*)-pen-OMe}$_2$], *via* partial chelate dissociation and without geometrical isomerisation. SN = (*S*)-penicillaminate methyl ester

mol^{-1} and $\Delta S^\ddagger = -52 \pm 3$ J K^{-1} mol^{-1}. The significantly negative entropies of activation for these processes are unexpected, given the suggested partial or total displacement of a ligand as the rate-determining step. In the case of the displacement of Ph_3PO by halide, the negative $\Delta S^\ddagger$ values were taken [37] to indicate extensive ordering of the solvent (CH_2Cl_2) molecules around the vacant co-ordination site and/or the leaving Ph_3PO group in the transition state. Such an effect would be more important for a strongly solvating solvent such as Me_2SO, consistent with the more negative $\Delta S^\ddagger$ value observed here, and thus we have tentatively included a Me_2SO molecule in the Scheme for the inversion process. A similar scheme

would appear to apply to the inversion of configuration about the molybdenum in *cis*-[MoO_2{(*R*)-cys-OMe}$_2$], where $\Delta G_{298}^{\ddagger}$, as determined [8] from the coalescence of the ^{95}Mo resonances for the compound in dimethylformamide solution, is 63 kJ mol^{-1}.

Stereochemical non-rigidity has been observed by ^{1}H n.m.r. for β-diketonate complexes of *cis*-dioxomolybdenum(VI); [38,39] in these processes the alkyl substituents at either end of the ligand (*cis* or *trans* to the terminal oxo-ligands) are rendered equivalent by chemical exchange in a process that is probably intramolecular. For *cis*-[MoO_2(pd)$_2$] (pd = pentane-2,4-dionate) in $CHCl_3$ or benzene solution, $\Delta H^{\ddagger}$ = 51.9 or 68.6 kJ mol^{-1} and $\Delta S^{\ddagger}$ = 59 or 18 J K^{-1} mol^{-1}, respectively.[38] In the case of *cis*-[MoO_2(tmhd)$_2$] (tmhd = 2,2,6,6-tetramethylheptane-3,5-dionate) in CH_2Cl_2 solution, only the $\Delta H^{\ddagger}$ value (58.6 kJ mol^{-1}) was determined and a twisting mechanism was favoured, but a mechanism involving Mo–O(C) bond rupture could not be excluded.[39]

An inversion mechanism involving total (rather than partial) dissociation of a ligand from *cis*-[MoO_2{(*S*)-pen-OMe}$_2$] has not been experimentally excluded. This is considered to be most unlikely, since the relatively low enthalpy of activation observed makes such a mechanism, involving the cleavage of Mo–N *and* Mo–S bonds, implausible.

Acknowledgements

We thank the S.E.R.C. for the award of a studentship (to I. B.), the Verband der Chemischen Industrie for financial support (to W. C.), Dr. B. E. Mann of the S.E.R.C. n.m.r. service at the University of Sheffield for recording n.m.r. spectra, and Dr. C. I. Watt for considerable assistance with the kinetic studies.

References

1 E. I. Stiefel, *Prog. Inorg. Chem.*, 1977, **22**, 1.
2 'Molybdenum and Molybdenum-Containing Enzymes,' ed. M. P. Coughlan, Pergamon Press, New York, 1980 and refs. therein.
3 C. D. Garner, *Coord. Chem. Rev.*, 1982, **45**, 153.
4 J. T. Spence, *Coord. Chem. Rev.*, 1983, **48**, 59.
5 J. Weber and C. D. Garner, *Inorg. Chem.*, 1980, **19**, 2206; C. D. Garner, N. C. Howlader, F. E. Mabbs, P. M. Boorman, and T. J. King, *J. Chem. Soc., Dalton Trans.*, 1978, 1350 and refs. therein.
6 R. Durant, C. D. Garner, M. R. Hyde, and F. E. Mabbs, *J. Chem. Soc., Dalton Trans.*, 1977, 955; P. M. Boorman, C. D. Garner, and F. E. Mabbs, *J. Chem. Soc., Dalton Trans.*, 1975, 1299 and refs. therein.
7 C. D. Garner, I. Buchanan, D. Collison, F. E. Mabbs, T. G. Porter, and C. H. Wynn, Proceedings of the Fourth International Conference on the Chemistry and Uses of Molybdenum, eds. H. F. Barry and P. C. H. Mitchell, Climax Molybdenum Company, Ann Arbor, Michigan, 1982, pp. 163—168.
8 I. Buchanan, M. R. Minelli, M. T. Ashby, T. J. King, J. H. Enemark, and C. D. Garner, *Inorg. Chem.*, 1984, **23**, 495.
9 T. G. Porter, Ph.D. Thesis, University of Manchester, 1981.
10 S. P. Cramer, R. Wahl, and K. V. Rajagopalan, *J. Am. Chem. Soc.*, 1981, **103**, 7721.
11 L. R. Melby, *Inorg. Chem.*, 1969, **8**, 349.
12 A. Kay and P. C. H. Mitchell, *J. Chem. Soc. A*, 1970, 2421.
13 W. Clegg, *Acta Crystallogr., Sect. A*, 1981, **37**, C313.
14 W. Clegg, *Acta Crystallogr., Sect. A*, 1981, **37**, 22.
15 S. C. Abrahams and E. T. Keeve, *Acta Crystallogr., Sect. A*, 1971, **27**, 157.
16 W. C. Hamilton, 'International Tables for *X*-Ray Crystallography,' Kynoch Press, Birmingham, 1974, vol. 4, p. 293.
17 D. Rogers, *Acta Crystallogr., Sect. A*, 1981, **37**, 734.
18 J. M. Berg, K. O. Hodgson, S. P. Cramer, J. L. Corbin, A. Elsberry, N. Pariyadath, and E. I. Stiefel, *J. Am. Chem. Soc.*, 1979, **101**, 2774.
19 K. Yamanouchi and J. H. Enemark, *Inorg. Chem.*, 1979, **18**, 1626.
20 E. I. Stiefel, K. F. Miller, A. E. Bruce, J. L. Corbin, J. M. Berg, and K. O. Hodgson, *J. Am. Chem. Soc.*, 1980, **102**, 3624.
21 A. Bruce, J. L. Corbin, P. L. Dahlstrom, J. R. Hyde, M. Minelli, E. I. Stiefel, J. T. Spence, and J. Zubieta, *Inorg. Chem.*, 1982, **21**, 917.
22 D. L. Kepert, *Prog. Inorg. Chem.*, 1977, **23**, 1.
23 IUPAC Commission on the Nomenclature of Inorganic Chemistry, Copenhagen, 1970; K. A. Jensen (Chairman), *Pure Appl. Chem.*, 1971, **28**, 1.
24 A. Bartecki, *Chem. Zvesti*, 1965, **19**, 161; A. Bartecki and D. Dembicka, *Rocz. Chem.*, 1965, **39**, 1783.
25 F. W. Moore and R. E. Rice, *Inorg. Chem.*, 1968, **7**, 2510.
26 A. Kay and P. C. H. Mitchell, *J. Chem. Soc., Dalton Trans.*, 1973, 1388.
27 M. Gullotti, A. Pasini, G. M. Zanderighi, G. Ciani, and A. Sironi, *J. Chem. Soc., Dalton Trans.*, 1981, 902.
28 S. Gutteridge and R. C. Bray, in 'Molybdenum and Molybdenum-Containing Enzymes,' ed. M. P. Coughlan, Pergamon Press, Oxford, 1980, pp. 223—239; R. C. Bray, *Adv. Enzymol. Relat. Areas Mol. Biol.*, 1980, **51**, 107.
29 R. J. Abraham and P. Loftus, 'Proton and Carbon-13 N.M.R. Spectroscopy: An Integrated Approach,' Heyden, London, 1973.
30 L. Flohe, E. Breitmaier, W. A. Günzler, W. Völter, and G. Jung, *Hoppe-Seyler's Z. Physiol. Chem.*, 1972, **353**, 1159.
31 K. A. Christensen, P. E. Miller, M. Minelli, T. W. Rockway, and J. H. Enemark, *Inorg. Chim. Acta*, 1981, **56**, L27.
32 A. Allerhand, H. S. Gutowsky, J. Jonas, and R. A. Meinzer, *J. Am. Chem. Soc.*, 1966, **88**, 3185; H. O. House, R. A. Latham, and G. M. Whitesides, *J. Org. Chem.*, 1967, **32**, 2481.
33 Curve-fitting routine NLR 1, 'Applied Statistics Programs. Vol. 2: Regression Analysis Program Manual,' University of Manchester Regional Computer Centre, 1980.
34 Program JUDY, Dr. C. I. Watt, Chemistry Department, Manchester University.
35 J. F. Bunnett, 'Techniques of Organic Chemistry. Vol. 3: Rates and Mechanisms of Reactions,' ed. A. Weisseberger, Interscience, New York, 1961, pp. 177—283.
36 F. Basolo and R. G. Pearson, 'Mechanisms of Inorganic Reactions: A Study of Metal Complexes in Solution,' 2nd edn., Wiley, New York, 1968, ch. 4 and refs. herein; R. H. Holm, 'Dynamic Nuclear Magnetic Resonance Spectroscopy,' eds. L. M. Jackman and F. A. Cotton, Academic Press, New York, 1975, pp. 317—376.
37 C. D. Garner, M. R. Hyde, F. E. Mabbs, and V. I. Routledge, *J. Chem. Soc., Dalton Trans.*, 1975, 1175.
38 B. M. Craven, K. C. Ramey, and W. B. Wise, *Inorg. Chem.*, 1971, **10**, 2626.
39 T. J. Pinnavaia and W. R. Clements, *Inorg. Nucl. Chem. Lett.*, 1971, **7**, 1127.

Received 25*th July* 1983; *Paper* 3/1275